Thin Solid Films 542 (2013) 348–354

Contents lists available at SciVerse ScienceDirect

Thin Solid Films

journal homepage: www.elsevier.com/locate/tsf

Magnetoresistance and anomalous Hall effect of reactive sputtered polycrystalline $Ti_{1-x}Cr_xN$ films

X.F. Duan [a], W.B. Mi [a,*], Z.B. Guo [b], H.L. Bai [a]

[a] Tianjin Key Laboratory of Low Dimensional Materials Physics and Preparation Technology, Institute of Advanced Materials Physics, Faculty of Science, Tianjin University, Tianjin 300072, China
[b] Core Labs, King Abdullah University of Science and Technology (KAUST), Thuwal 23955-6900, Saudi Arabia

ARTICLE INFO

Article history:
Received 4 September 2012
Received in revised form 11 June 2013
Accepted 20 June 2013
Available online 2 July 2013

Keywords:
Nitrides
Magnetic thin films
Magnetoresistance
Anomalous Hall effect
Reactive sputtering

ABSTRACT

The reactive-sputtered polycrystalline $Ti_{1-x}Cr_xN$ films with $0.17 \le x \le 0.51$ are ferromagnetic and at $x = 0.47$ the Curie temperature T_C shows a maximum of ~120 K. The films are metallic at $0 \le x \le 0.47$, while the films with $x = 0.51$ and 0.78 are semiconducting-like. The upturn of resistivity below 70 K observed in the films with $0.10 \le x \le 0.47$ is from the effects of the electron–electron interaction and weak localization. The negative magnetoresistance (MR) of the films with $0.10 \le x \le 0.51$ is dominated by the double-exchange interaction, while at $x = 0.78$, MR is related to the localized magnetic moment scattering at the grain boundaries. The scaling $\rho_{xy}^A/n \propto \rho_{xx}^{2.19}$ suggests that the anomalous Hall effect in the polycrystalline $Ti_{1-x}Cr_xN$ films is scattering-independent.

1. Introduction

The transition metal nitrides TiN and CrN are excellent in high hardness and mechanical strength, and have been used in the cutting tools and hard coatings industry over the last twenty years [1]. Moreover, TiN has a low resistivity of 10^{-5} Ω cm showing a superconductive character at ~5 K and CrN is semiconducting with a magnetic transition from paramagnetism to antiferromagnetism at a Néel temperature of ~280 K [2–5]. The $Ti_{1-x}Cr_xN$ solid solutions have been found not to further increase hardness [6] but are interesting for their surprising ferromagnetism that was first discovered by Aivazov and Gurov in 1975 [7]. Thirty years later, the magnetic and electrical transport properties of the $Ti_{1-x}Cr_xN$ samples were reinvestigated by Inumaru et al. [8–10]. A large magnetoresistance (MR) of 5%–7% at 5 T was found in the $Ti_{0.5}Cr_{0.5}N$ solid solutions, suggesting the possibility of using a nitride material in spintronics [9,10]. Subsequently, Alling et al. [11,12] investigated the magnetism of the $Ti_{1-x}Cr_xN$ solid solutions by first-principle calculations, and qualitatively confirmed the experimental findings of ferromagnetic ordering in the Ti-rich regime [9,10].

Previously, we have systematically investigated the magnetic and transport properties of the epitaxial $Ti_{1-x}Cr_xN$ films, observing a series of characteristics dominated by the Cr–N–Cr double-exchange interaction, which is similar to the colossal magnetoresistance manganites [13]. It is worth noting that polycrystalline perovskite manganites exhibit a large MR at a lower saturation field than epitaxial films due to the spin-polarized tunneling at the grain boundaries (GBs) [14,15]. This phenomenon inspires us study the polycrystalline $Ti_{1-x}Cr_xN$ films so as to clarify the role of GBs on the spin-dependent transport properties.

Moreover, in our previous work, the anomalous Hall effect (AHE) of the epitaxial $Ti_{1-x}Cr_xN$ films shows a quadratic dependence of the AHE resistivity ρ_{xy}^A on the longitudinal resistivity ρ_{xx} [13]. However, it is also necessary to investigate the scaling relation between ρ_{xy}^A and ρ_{xx} in the polycrystalline $Ti_{1-x}Cr_xN$ films in order to clarify the influence of the carrier scatterings by GBs on AHE.

In this paper, polycrystalline $Ti_{1-x}Cr_xN$ films with $0 \le x \le 0.78$ were fabricated by reactive facing-target sputtering. The negative MR observed in the films with $0.10 \le x \le 0.51$ is dominated by the double-exchange interaction, while MR of the film with $x = 0.78$ is related to the localized magnetic moment scattering at the GBs. The scaling $\rho_{xy}^A/n \propto \rho_{xx}^{2.19}$ suggests a scattering-independent AHE in the polycrystalline $Ti_{1-x}Cr_xN$ films.

2. Experimental details

Polycrystalline $Ti_{1-x}Cr_xN$ films with different Cr atomic fractions (x) were grown on polished Si(100) and glass substrates by dc reactive facing-target sputtering in a gas mixture of Ar (5N) and N_2 (5N). The targets were a pair of pure Ti (5N) targets on which the pure Cr (5N) chips were placed. The Cr atomic fraction was adjusted by change of the amount of Cr chips. The base pressure was lower than 8.0×10^{-6} Pa, and the total sputtering pressure was kept at 1.0 Pa with a flow rate of 50-sccm Ar and 50-sccm N_2. The substrate

* Corresponding author. Tel.: +86 22 27406991; fax: +86 22 27403425.
E-mail address: miwenbo@tju.edu.cn (W.B. Mi).

0040-6090/$ – see front matter © 2013 Elsevier B.V. All rights reserved.
http://dx.doi.org/10.1016/j.tsf.2013.06.068

temperature was kept at 550 °C during the sputtering. The film thickness was ~120 nm determined by a Dektak 6M surface profiler. The Cr and Ti atomic fractions were measured by an energy-dispersive X-ray spectrometer (EDAX Genesis XM2, working at 15 kV) with which a scanning electron microscope was equipped. The microstructure was characterized by an X-ray diffractometer (XRD, D/max-2500×, Cu Kα, λ = 1.5406 Å), where the θ–2θ scan configuration was used, and a transmission electron microscope (TEM, Tecnai G2 F20 S-Twin) at an operating voltage of 200 kV. For cross-section TEM observations, the samples were pasted face-to-face and then thinned below 100 nm. The magnetic properties were investigated using a Quantum Design superconducting quantum interference device-vibrating sample magnetometer and MR was measured by a Quantum Design physical property measurement system using a standard four-probe configuration. The Hall resistivity ρ_{xy} was calculated from $V_{xy}d/I$, where V_{xy} was the transverse voltage, d was the film thickness, and I was the applied DC current. For excluding the effect of the contact resistance, the true Hall resistivity was obtained by subtracting the Hall resistivity measured at the negative magnetic fields from that measured at the positive magnetic fields, then divided by 2 because MR is symmetric on the axis of resistivity.

3. Results and discussion

Fig. 1 shows the XRD patterns of the polycrystalline $Ti_{1-x}Cr_xN$ films on Si(100) substrates. The main diffraction peaks located at 36.70°, 42.68° and 61.87° are from the face-centered-cubic TiN(111), (200) and (220) planes, respectively. The peaks are consistent with the standard XRD patterns of TiN powders and no Cr-related secondary phases or impurities were detected in all of the films. Except for the pure TiN film, the intensity of the $Ti_{1-x}Cr_xN(111)$ peaks is much larger than those of the $Ti_{1-x}Cr_xN(200)$ and (220) peaks, implying that the films prefer to grow along the [111] orientation. Furthermore, the shift of the $Ti_{1-x}Cr_xN(111)$ diffraction peak to higher angle, from 36.70° at $x = 0$ to 36.99° at $x = 0.78$, indicates lattice shrinking with the increasing x. The lattice shrinking should be attributed to the substitution of the larger Ti atoms (atom radius 0.61 Å) with the smaller Cr atoms (atom radius 0.52 Å).

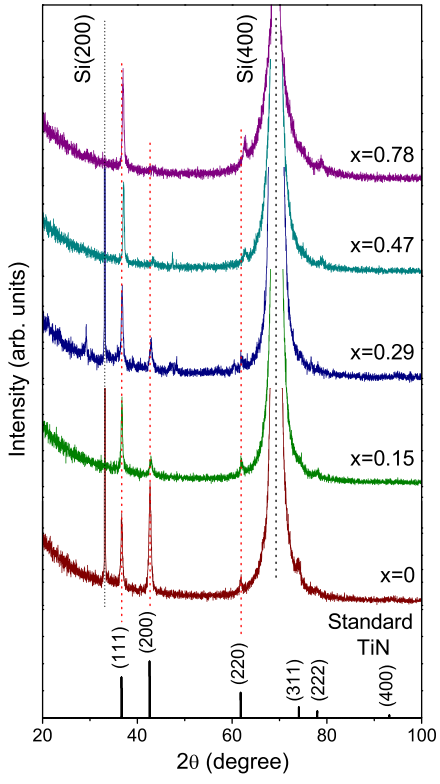

Fig. 1. XRD patterns of the polycrystalline $Ti_{1-x}Cr_xN$ films deposited on Si(100) substrates.

In order to further characterize the microstructure of the polycrystalline $Ti_{1-x}Cr_xN$ films, the high-resolution TEM analysis was carried out at the $Ti_{0.53}Cr_{0.47}N$/substrate interface. Shown in Fig. 2(a) is the low magnification image of the $Ti_{0.53}Cr_{0.47}$ N/Si interface, from which we can see the columnar growth of the film with a thickness of ~120 nm. The high-resolution TEM image in Fig. 2(b) shows different lattice orientations, manifesting that the films are polycrystalline. The d spacings indexed in the figure are from the $Ti_{0.53}Cr_{0.47}N(111)$ and (200) planes, corresponding to two major diffraction peaks in XRD. An amorphous native silicon oxide layer of ~2 nm in thickness is also observed in the image.

The in-plane M–H curves of the $Ti_{1-x}Cr_xN$ films measured at 30 K are plotted in Fig. 3(a). The typical hysteresis loops indicate that the films with $0.35 \le x \le 0.51$ are ferromagnetic at 30 K with coercivity less than 4 kA/m. The top-left inset shows the x-dependent saturation magnetization (M_s) at 30 K. M_s increases with increasing x from 0.17 to 0.47, and reaches a maximum of 106 kA/m at $x = 0.47$. When x further increases, M_s decreases sharply. M_s of the film with $x = 0.51$ is only 57 kA/m, nearly half of the maximum M_s, and the film with $x = 0.78$ is not ferromagnetic (not shown here). The rapid decrease of M_s at $x > 0.47$ is attributed to the strong decrease of double-exchange strengths in the Cr-rich region, which is consistent with the results obtained by Inumaru et al. [9,10]. The bottom-right inset of Fig. 3(a) presents the M^2–H/M curves (Arrott plots) of the film with $x = 0.47$ at 15–175 K. The Arrott curve passes through the origin at 125 K, which is an indication of ferromagnetic transition temperature.

Fig. 3(b) shows the M–T curves of the $Ti_{1-x}Cr_xN$ films with different x under a magnetic field of 40 kA/m. The film with $x = 0.47$ shows the highest Curie temperature (T_C) of ~120 K, roughly consistent with the Arrott result. At $x = 0.43$, T_C is a bit lower than 120 K, while that of the films with $x = 0.35$ and 0.51 is ~100 K. The zero field cooling (ZFC) and field cooling (FC) curves for the film with $x = 0.47$ are shown in the top-right inset of Fig. 3(b). The bifurcation of ZFC and FC curves at ~40 K, followed by a sharp decline in ZFC curve and a upturn in FC curve below 15 K, indicates a spin-glass-like transition in the film [16].

Fig. 4(a) presents the temperature dependence of the normalized resistivity $\rho(T)/\rho(305\ K)$ of the polycrystalline $Ti_{1-x}Cr_xN$ films. The pure TiN film has the conductance characteristics of normal metals from 305 to 5 K, and below 5 K superconductive characteristics appear, as shown in the bottom-right inset of Fig. 4(a), irrespective of the existence of grain boundaries in the polycrystalline film. As Cr atoms are doped, a resistivity minimum ρ_{min} at low temperatures appears, which can be observed in the films with $0.10 \le x \le 0.47$. The $\rho(T)$ dependence exhibits a sharp change of slope near T_C in the films with $0.35 \le x \le 0.47$ as a result of the reduced spin-disorder scattering. Such a behavior of $\rho(T)$ is a typical characteristic of ferromagnetic metals. Negative temperature coefficients of resistivity (TCR = $d\rho / dT$) are observed for the films with $x = 0.51$ and 0.78 in a very wide temperature range, showing a semiconductor-like conductance behavior.

Shown in the top inset of Fig. 4(a) is the room-temperature resistivity of the films. Resistivity is in the range of 10^{-5}–10^{-4} Ω cm reaching a maximum at $x = 0.51$. Resistivity increases with the substitution of Cr can be explained by the fact that the resistivity of CrN (10^{-3} Ω cm) is two-order larger than the resistivity of pure TiN (10^{-5} Ω cm), while the further decrease at $x = 0.78$ may be due to the film deposition by sputtering being a non-equilibrium process. The room-temperature resistivity of the pure TiN film is ~53 μΩ cm, slightly larger than that of reported data (~40 μΩ cm) [17].